Physics of the Solid State, Vol. 45, No. 1, 2003, pp. 41–45. Translated from Fizika Tverdogo Tela, Vol. 45, No. 1, 2003, pp. 42–45.
Original Russian Text Copyright © 2003 by Aleksandrov, Sorokin, Glushkov, Bezmaternykh, Burkov, Belushchenko.

SEMICONDUCTORS AND DIELECTRICS

Electromechanical Properties and Anisotropy of Acoustic Wave Propagation in CuB_2O_4 Copper Metaborate

K. S. Aleksandrov*, B. P. Sorokin, D. A. Glushkov**, L. N. Bezmaternykh*,
S. I. Burkov**, and S. V. Belushchenko***

** Kirensky Institute of Physics, Siberian Division, Russian Academy of Sciences,
Akademgorodok, Krasnoyarsk, 660036 Russia*

*** Krasnoyarsk State University, Krasnoyarsk, 660041 Russia*

e-mail: bsorokin@lan.krasu.ru

Received March 12, 2002

Abstract—The propagation of bulk acoustic waves in single-crystal CuB_2O_4 copper metaborate is studied. The elastic, piezoelectric, and dielectric constants are calculated. The anisotropy in the parameters of bulk acoustic wave propagation in this crystal are determined. *© 2003 MAIK “Nauka/Interperiodica”.*

1. The interest in undertaking a coordinated investigation of the properties of single-crystal copper oxyborates has been spurred by recent studies on their low-temperature magnetism [1–6]. The most comprehensive data, including determination of the magnetic structure using neutron diffraction [4], were obtained for the CuB_2O_4 copper metaborate. This tetragonal noncentrosymmetric crystal [7], belonging to space group $D_{2d}^{12} = I\bar{4}2d$, with the lattice parameters a = 11.528 Å and c = 5. 607 Å, remains paramagnetic down to 21 K. At lower temperatures, the crystal transfers to the antiferromagnetic state and its weak ferromagnetic moment of approximately 0.56 emu/g is accounted for by the two coupled sublattices being slightly misoriented [1]. Below 10 K, the compound undergoes a second phase transition to an incommensurate spiral structure, which is due primarily to the Dzyaloshinsky–Moriya antisymmetric exchange interaction [5]. Optical absorption spectra of CuB_2O_4 are discussed in [8].

At the same time, we are not aware of any publications dealing with such properties as the elasticity and piezoelectric effect of this crystal. The present paper reports on a measurement of the bulk acoustic wave (BAW) velocities and determination of the elastic, dielectric, and piezoelectric constants of this crystal, as well as on a calculation of the anisotropy in the BAW parameters.

Single crystals of copper metaborate, up to 10–15 cm^3 in volume, were grown, as in [9], from lithium borate melt solutions diluted by MoO_3. In such melt solutions, the growing face also maintains stability with a seed growing from the melt-solution surface, which made possible a stable Kyropoulos process with a lowered temperature in the interval 920–850°C.

2. BAW propagation in a crystal is described by the Green–Christoffel equation [10], whose solution yields the velocities and polarization vectors of BAWs propagating in a given crystal direction. Expressions for BAW velocities, which, in general, are combinations of elastic, piezoelectric, and dielectric constants, are presented in Table 1 for some directions in crystals of point symmetry group $\bar{4}2m$, to which the copper metaborate CuB_2O_4 belongs.

The BAW velocities in CuB_2O_4 were measured using the pulsed ultrasonic technique (30 MHz) [10] based on measuring the time of ultrasonic pulse propagation in a sample. This method ensures an accuracy of not worse than 10^{-4} in absolute measurements and a sensitivity of 10^{-6} in relative measurements. The CuB_2O_4 samples, shaped as polished-face rectangular parallelepipeds with linear dimensions ≈1 cm, were cut from the same boule. The crystallographic orientation of the samples was checked with an x-ray diffractometer to within ±3′. The sample orientations are shown in Fig. 1. The results of the BAW velocity measurements are listed in Table 2.

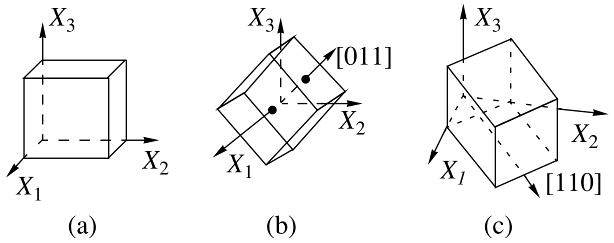

(a) (b) (c)

Fig. 1. Sample orientation. (a) Sample *1*, (b) sample *2*, and (c) sample *3*.

1063-7834/03/4501-0041$24.00 © 2003 MAIK “Nauka/Interperiodica”

Table 1. BAW velocities and electromechanical constants in crystals of $\bar{4}2m$ symmetry

Direction of propagation	Type of wave	Direction of polarization vector	ρV^2
[100]	L	[100]	C_{11}^E
	S	[010]	C_{66}^E
	S	[001]	C_{44}^E
[001]	L	[001]	C_{33}^E
	S		C_{44}^E
[110]	L	[110]	$1/2(C_{11}^E + C_{12}^E) + C_{66}^E$
	S	[001]	$C_{44}^E + \frac{e_{14}^2}{\varepsilon_{11}^\eta}$
	S	$[\bar{1}10]$	$1/2(C_{11}^E - C_{12}^E)$
[011]	S	[100]	$0.19C_{66}^E + 0.81C_{44}^E + \frac{0.16(e_{14} + e_{36})^2}{0.19\varepsilon_{11}^\eta + 0.81\varepsilon_{33}^\eta}$
	QS		$1/2(0.19C_{11}^E + 0.81C_{33}^E + C_{44}^E)$ $- 1/2\sqrt{[0.19(C_{11}^E - C_{44}^E) + 0.81(C_{44}^E - C_{33}^E)]^2 + 0.62(C_{44}^E + C_{13}^E)^2}$

Note: L is longitudinal, S shear, and QS quasi-shear mode.

The dielectric permittivities of mechanically free samples ε_{11}^σ and ε_{33}^σ were derived from the capacity of planar capacitors prepared from *X*- and *Z*-cut plates; the capacity was measured with an E8–4 high-precision semiautomatic bridge (1 kHz). These data were used to determine the elastic and piezoelectric constants of CuB_2O_4 from the BAW velocities.

Table 2. BAW velocities in single-crystal CuB_2O_4 (20°C)

Direction of propagation	Type of wave	Direction of polarization vector	Velocity, m/s
[100]	L	[100]	9917.6 ± 0.1
	S	[010]	4867.7 ± 0.1
	S	[001]	5307.0 ± 0.5
[001]	L	[001]	8882.5 ± 1.2
	S		5307.0 ± 0.5
[110]	L	[110]	9227.3 ± 1.4
	S	[001]	5317.3 ± 0.3
	S	$[\bar{1}10]$	6073.4 ± 0.2
[011]	S	[100]	5234.9 ± 1.1
	QS		5471.9 ± 1.3

3. As seen from Table 1, the signs of the piezoelectric constants e_{14} and e_{36} cannot be determined from the BAW velocities alone. The relative sign of these constants has to be found independently. It should be pointed out that crystals belonging to point symmetry group $\bar{4}2m$ permit the existence of two inequivalent sets of crystallographic coordinate systems (CCSs). In choosing the CCS, we were guided by the rules proposed in [11], according to which the proper CCS is that in which the condition for the piezoelectric modulus $d_{36} > 0$ is met. Therefore, we chose the proper CCS and analyzed the signs of the piezoelectric constants by using the static direct piezoelectric effect.

Consider the behavior of a sample oriented as shown in Fig. 1c under the application of uniaxial mechanical compression along the [011] direction. The equation of state for this case can be written as

$$D'_i = d'_{ikl}\sigma'_{kl}, \tag{1}$$

where all quantities are defined relative to the “rotated” coordinate system (Fig. 2a). In this coordinate system, the mechanical stress tensor corresponding to uniaxial compression has the form

$$\sigma'_{kl} = \begin{pmatrix} -p & 0 & 0 \\ 0 & 0 & 0 \\ 0 & 0 & 0 \end{pmatrix} \tag{2}$$

in the case of compression along the X'_1 axis and

$$\sigma'_{kl} = \begin{pmatrix} 0 & 0 & 0 \\ 0 & -p & 0 \\ 0 & 0 & 0 \end{pmatrix} \tag{3}$$

for compression along the X'_2 axis. The pressure is assumed to be negative. Then, the electric induction vector should have only one nonzero component, either

$$D'_3 = -d'_{31}p_{X'_1} = -\frac{1}{2}d_{36}p_{X'_1} \tag{4}$$

or

$$D'_3 = -d'_{32}p_{X'_2} = \frac{1}{2}d_{36}p_{X'_2}. \tag{5}$$

Thus, by measuring the sign of the charges produced by the direct piezoelectric effect at the sample faces perpendicular to the X'_3 axis under uniaxial mechanical stress along X'_1 or X'_2 and assuming $d_{36} > 0$, one can choose the direction of axes of the original coordinate system in a given sample. After this, because all the samples were prepared from the same boule and their mutual orientation is known, we fix the axes of the original CCS in sample *2* (Fig. 1b). Following the same reasoning, we find that the nonzero component of the electric induction vector in the case of uniaxial mechanical compression applied to sample *2* along X'_2 (Fig. 2b) is

$$D'_1 = -kd_{14}p_{X'_2}, \tag{6}$$

where k is a positive coefficient depending on the rotation angle of the coordinate system. Measurements performed in accordance with Eqs. (4)–(6) showed that in CuB_2O_4 for $d_{36} > 0$ the inequality $d_{14} > 0$ is met.

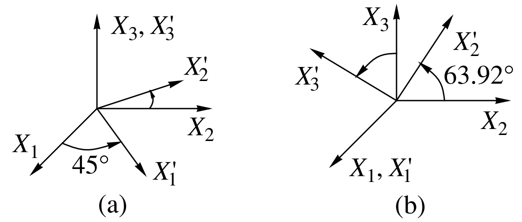

Fig. 2. Rotated coordinate systems (a) for sample *3* and (b) for sample *2*.

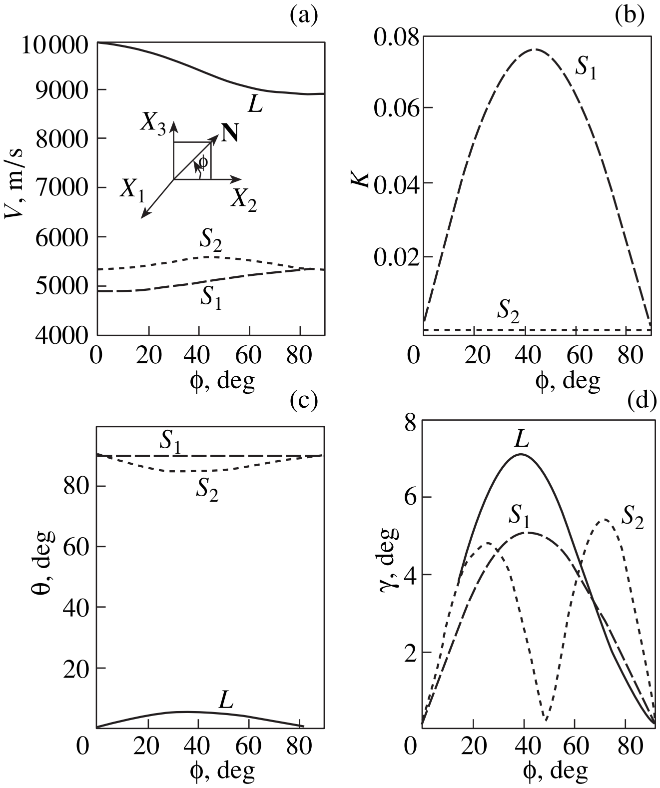

Fig. 3. Anisotropy in the BAW propagation parameters for CuB_2O_4 in the (100) plane. (a) BAW phase velocities, (b) electromechanical coupling coefficients, (c) angles between the polarization vector and direction of BAW propagation, and (d) angles of BAW energy flow deviation. **N** is the wave normal vector.

Table 3. Material constants of single-crystal CuB_2O_4 (20°C)

$C^E_{\lambda\mu}$, 10^{10} Pa	C^E_{11}	C^E_{12}	C^E_{13}	C^E_{33}	C^E_{44}	C^E_{66}
	39.54 ± 0.01	9.86 ± 0.02	10.56 ± 0.02	31.72 ± 0.01	11.32 ± 0.01	9.53 ± 0.01
ρ, kg/m^3 [7]	$e_{i\lambda}$, C/m^2	e_{14}	e_{36}	ε^σ_{ij}	ε^σ_{11}	ε^σ_{33}
4020		0.14 ± 0.01	0.22 ± 0.01		6.09 ± 0.05	6.14 ± 0.05

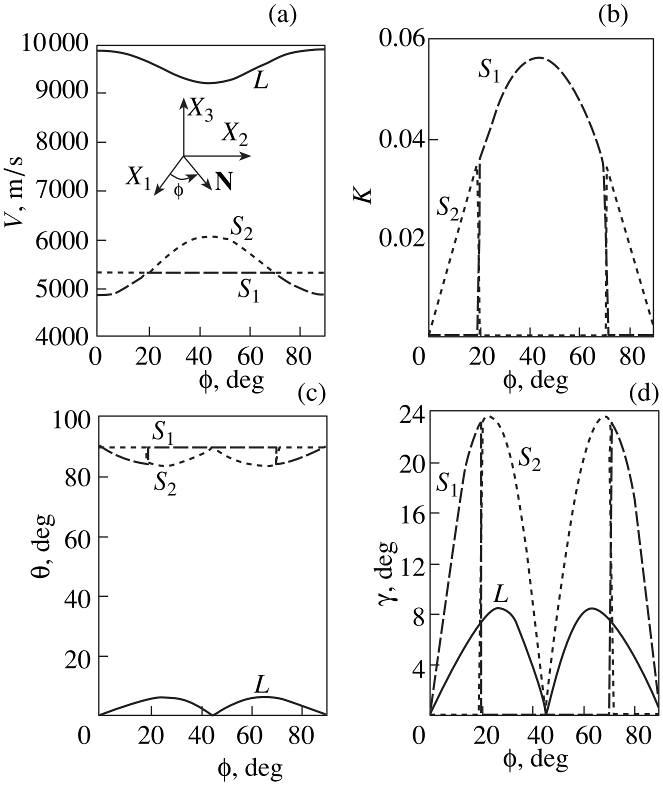

Fig. 4. Anisotropy in the BAW propagation parameters for CuB_2O_4 in the (001) plane. (a) BAW phase velocities, (b) electromechanical coupling coefficients, (c) angles between the polarization vector and direction of BAW propagation, and (d) angles of BAW energy flow deviation. **N** is the wave normal vector.

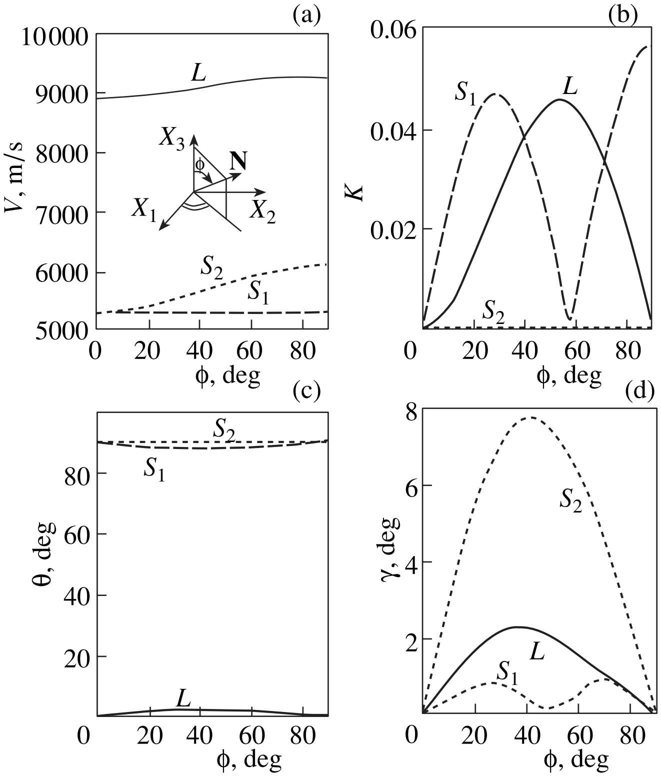

Fig. 5. Anisotropy in the BAW propagation parameters for CuB_2O_4 in the $(1\bar{1}0)$ plane. (a) BAW phase velocities, (b) electromechanical coupling coefficients, (c) angles between the polarization vector and direction of BAW propagation, and (d) angles of BAW energy flow deviation. **N** is the wave normal vector.

The relation connecting the piezoelectric constants with piezoelectric moduli presented in [11] reduces in our case to

$$e_{14} = d_{14}C_{44}^E, \quad (7)$$

$$e_{36} = d_{36}C_{66}^E. \quad (8)$$

Because the elastic constants are $C_{44} > 0$ and $C_{66} > 0$ (see Tables 1, 2), the piezoelectric constants are $e_{14} > 0$ and $e_{36} > 0$.

The Mohs hardness of the copper metaborate is more than seven units (a single crystal scratches quartz). The deep blue color, chemical stability, homogeneity, and fairly large dimensions of this crystal make it attractive as material for use in jewelry; its refractive indices $N_o = 1.69$ and $N_e = 1.582$ were determined in [12].

4. The material constants thus obtained (Table 3) were used to calculate the anisotropy in the BAW parameters for some planes of the CuB_2O_4 crystal. The results are presented in Figs. 3–5. Figure 3a shows the anisotropy of the BAW velocities for propagation in directions lying in the (100) plane. The velocities of longitudinal waves in this plane reach a maximal value, which is relatively high (about 10000 m/s), in the X_1 (X_2) directions. The X_3 direction (fourfold inversion axis) is the acoustic axis. Figure 3b displays the anisotropy of the electromechanical coupling coefficient (ECC). Only the slow shear wave polarized along [100] is accompanied by the longitudinal piezoelectric activity. For propagation at an angle $\phi \approx 44°$, the ECC for this mode reaches a maximum value $k \approx 7.6\%$. This value characterizes the copper metaborate as a weak piezoelectric crystal. Figure 3c shows the BAW polarization angles, which can be used to determine the directions of the “pure” modes. In this plane, pure modes propagate along crystallographic axes. Figure 3d illustrates the angles of the BAW energy flow deviation. Shown graphically in Fig. 4 are the results of similar calculations made for the (001) plane. Note the presence of acoustic axes which do not coincide with the crystallographic directions and lie at angles $\phi \approx 20°$ and 70°. As one crosses the acoustic axis, the polarization vector solutions, as it were, become replaced; more specifically, the shear-wave polarization vectors rotate by 90°. The shear wave polarized along [001] is an elastically isotropic wave. As follows from Fig. 5 [the $(1\bar{1}0)$

plane], the longitudinal mode, as well as the slow shear wave, is accompanied by the longitudinal piezoelectric activity.

ACKNOWLEDGMENTS

This study was supported by the Russian Foundation for Basic Research (project no. 00-15-96790) and the Federal Program "Integration" (project no. 69).

REFERENCES

1. G. Petrakovskii, D. Velikanov, A. Vorotinov, *et al.*, J. Magn. Magn. Mater. **205**, 105 (1999).
2. G. A. Petrakovskiĭ, A. D. Balaev, and A. M. Vorotynov, Fiz. Tverd. Tela (St. Petersburg) **42** (2), 313 (2000) [Phys. Solid State **42**, 321 (2000)].
3. G. A. Petrakovskiĭ, K. A. Sablina, D. A. Velikanov, *et al.*, Kristallografiya **45** (5), 926 (2000) [Crystallogr. Rep. **45**, 853 (2000)].
4. B. Roessli, J. Schefer, G. Petrakovskii, *et al.*, Phys. Rev. Lett. **86** (9), 1885 (2001).
5. G. A. Petrakovskiĭ, M. A. Popov, B. Roessli, and B. Ouladdiaf, Zh. Éksp. Teor. Fiz. **120** (4), 926 (2001) [JETP **93**, 809 (2001)].
6. H. Kageyama, K. Onizuka, T. Yamauchi, and Y. Ueda, J. Cryst. Growth **206**, 65 (1999).
7. M. Martinez-Ripoll, S. Martinez-Carrera, and S. Garcia-Blanco, Acta Crystallogr. B **27**, 677 (1971).
8. L. N. Bezmaternykh, A. M. Potseluĭko, E. A. Erlykova, and I. S. Édel'man, Fiz. Tverd. Tela (St. Petersburg) **43** (2), 297 (2001) [Phys. Solid State **43**, 309 (2001)].
9. L. N. Bezmaternykh, A. D. Vasil'ev, I. A. Gudim, *et al.*, in *Proceedings of the IX National Conference on Crystal Growth, Moscow, 2000*, p. 457.
10. M. P. Zaĭtseva, Yu. I. Kokorin, Yu. M. Sandler, V. M. Zrazhevskiĭ, B. P. Sorokin, and A. M. Sysoev, *Nonlinear Electromechanical Properties of Noncentrosymmetric Crystals* (Nauka, Novosibirsk, 1986).
11. Yu. I. Sirotin and M. P. Shaskolskaya, *Fundamentals of Crystal Physics* (Nauka, Moscow, 1979; Mir, Moscow, 1982).
12. G. K. Avdulaev, P. F. Rza-Zade, and S. Kh. Mamedov, Zh. Neorg. Khim. **27** (7), 1837 (1982).

Translated by G. Skrebtsov